
ACOUSTIC SIGNAL PROCESSING.
COMPUTER SIMULATION

Characterization of Cylindrical Ultrasonic Transducers Using Acoustic Holography

S. A. Tsysar^a, Y. D. Sinelnikov^b, and O. A. Sapozhnikov^{a, c}

^a *Physics Faculty, Moscow State University, Moscow, 119991 Russia*

^b *Sound Interventions, Inc., 25 Health Sciences Drive, Suite 201, Box 4201, Stony Brook, NY 11790, USA*

^c *Applied Physics Laboratory, University of Washington, Seattle, WA 98105, USA*

e-mail: sergey@acs366.phys.msu.ru

Received July 29, 2010

Abstract—We present the results of studying the vibrational velocity distribution over the surface of cylindrical ultrasound transducers by acoustic holography. We describe two approaches for acoustic holography: the spatial spectrum method and the Rayleigh integral method. In the case of cylindrical sources the spectral method has a specific feature in comparison to the case of quasi-plane sources: small-scale spectrum components having the form of evanescent (nonpropagating) waves near the source, turn into propagating waves at a certain distance from the source. The use of such a mixed type of waves makes it possible to increase the holographic resolution. To conduct holography of cylindrical sources by the Rayleigh integral method, a modification consisting in the superimposing of boundaries on the integration region is proposed. We present the results of numerical simulation and physical experiments on holography of small cylindrical piezoelectric transducers. We demonstrate that the proposed methods of holography make it possible to recover the vibration structure of source surfaces up to order of the wavelength scales.

DOI: 10.1134/S1063771011010167

INTRODUCTION

To increase the quality of ultrasound diagnostics and retain the highest selectivity of action in therapy, it is important to be able to calculate the spatiotemporal structure of the acoustic field. Obviously, any inaccuracy or error in using ultrasound in diagnostics and therapy increases the risks to patient health. Therefore, it is necessary to know the true field spatial distribution of medical transducers; in particular, for multi-element diagnostic antenna arrays, it is necessary to track the appearance and character of undesired side lobes and parasitic maxima; for devices of large wave dimensions applied in therapy and surgery, is necessary to calculate the most accurately the ultrasound intensity and the dimensions of the focal region. It is impossible to predict the fine spatial structure of acoustic fields without knowledge of the character of a transducer's surface vibrations. Whereas the characteristics of electronic devices (generators, amplifiers, oscilloscopes) can be easily measured and taken into account during measurements, the parameters of ultrasound transducers themselves are usually insufficiently known. Companies producing ultrasound transducers report only one-dimensional characteristics like frequency or impulse response as technical specifications; in the best case, the dimensional characteristic in the far field is given. Therefore, in practice, to describe the structure of the acoustic field of sources,

it is necessary to rush to certain conclusions with respect to the vibration structure of source surfaces. It is commonly accepted that the distribution of the normal component of the vibration speed on a transducer surface is uniform; i.e., the transducer vibrates like a hard piston. However, the true field distribution along the surface of piezoelectric ultrasound sources, as a rule, significantly deviates from a "piston" source [1, 2]. Therefore, the parameters of the entire system, calculated using a piston approximation (such as the directivity pattern, the location of the focus, the intensity at specific points, the degree of field symmetry, etc.) can noticeably differ from the actual parameters, which leads to errors that are frequently unacceptable for a number of applications.

To find the field on the source, acoustic holography is quite promising, which makes it possible to recover the vibration speed on the transducer surface. Using these data, we can calculate the acoustic field created by the transducer with a high degree of accuracy. The efficiency of this method for plane and spherically focused sources was confirmed in our previous works [2–4]. In medical applications and in hydroacoustics, in addition to the above, cylindrical ultrasound piezoelectric transducers are also used, the vibration speed distribution on the surface of which is unknown. An example of using cylindrical sources in ultrasound surgery is the method of treating atrial fibrillation, in which the high-frequency (on the order of 9 MHz)

cylindrical radiator produces a thermal action on the wall of a pulmonary vein is produced [5]. To successfully test, it is important to know the exact vibration speed distribution on the surface of the radiator.

The aim of this work is to study the vibration speed distribution on the surface of cylindrical ultrasound transducers by acoustic holography. It is shown that acoustic holography of sources can be implemented in several ways, among which two are the simplest and most effective. One of them is based on the use of the spatial spectral method (Fourier acoustics), and the second, on the principle of time reversal acoustics (TRA) and use of the Rayleigh integral.

FOURIER ACOUSTICS FOR HOLOGRAPHY OF CYLINDRICAL SOURCES

Using classical Fourier acoustics, the acoustic field expands over plane waves of different directions (angular spectrum method) [6]. When the measurement plane is located close to the source and is able to measure inhomogeneous waves, a unique feature of this method manifests itself, which makes it possible to recover the structure of the source with a spatial resolution less than the wavelength. The corresponding procedure of calculating back propagation is called “near-field acoustical holography¹” [7, 8]. When the measurement surface is located far from the source (distances on the order of several wavelengths or more), inhomogeneous waves are lost on the noise background and the spatial resolution of the method is limited by the usual diffraction limit (on the order of the wavelength). In this case, only an approximate solution to the inverse problem exists. Nevertheless, for the megahertz frequency range in liquids, this approximation is acceptable and gives high accuracy for a number of applications [2].

It is convenient to describe cylindrical sources and the acoustic fields created by them in cylindrical coordinates (r, φ, z) . We examine a cylinder of radius r_0 , the axis of which coincides with that of the cylindrical system of coordinates (Fig. 1). The cylinder radiates at frequency f a harmonic wave in which the acoustic pressure near the radiator is described by an unknown distribution $p(r_0, \varphi, z)$. In the linear case, for acoustic pressure $p(r, \varphi, z)$, the Helmholtz equation is justified:

$$\Delta p + k^2 p = 0, \quad (1)$$

where $k = \omega/c$ is the wavenumber and $\Delta = \partial^2/\partial r^2 + r^{-1}\partial/\partial r + \partial^2/\partial z^2 + r^{-2}\partial^2/\partial\varphi^2$ is the Laplace operator. The acoustic pressure on a cylindrical surface $r = \text{const}$ can be represented as a Fourier series over φ

¹ Strictly speaking, such holography is more properly called ultra-near-field holography, since the traditionally determined near field of a source extends to a distance $\sim D^2/\lambda$ (D is the source diameter and λ is the wavelength) and therefore for sources of large wave dimensions greatly exceeds the wavelength.

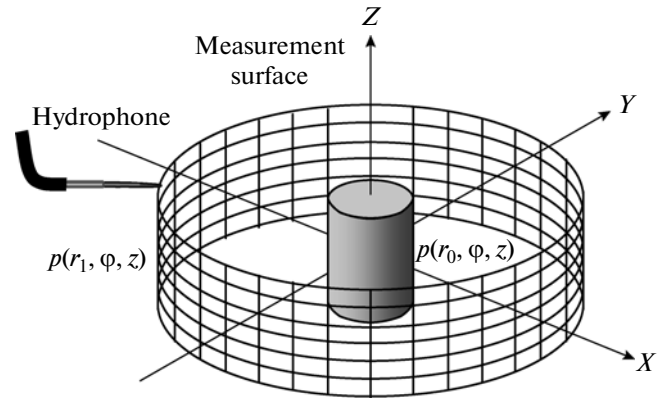


Fig. 1. Position of the radiating cylinder and measurement surface.

(due to field periodicity over the polar angle) and a Fourier integral over z [9]:

$$p(r, \varphi, z) = \frac{1}{2\pi} \sum_{m=-\infty}^{\infty} e^{im\varphi} \int_{-\infty}^{\infty} dk_z P_m(k_z; r) e^{ik_z z}. \quad (2)$$

Here, wave number k_z gives the spatial frequency in the direction of axis z and number m characterizes the oscillation frequency as a function of the polar angle (number m is equal to the number of periods of the chosen spectral component upon complete circumvention of the cylinder). Similarly to the case of plane sources, the spatial spectrum is an expansion of the field over plane waves of different directions, and representation (2) expresses the field of cylindrical sources in the form of superposition of helical waves, the wave fronts of which in the far field assume a conical shape [6]. The value of spectral amplitude $P_m(k_z; r)$ can be obtained applying inverse Fourier transform to both sides of expression (2):

$$P_m(k_z; r) = \frac{1}{2\pi} \int_0^{2\pi} d\varphi e^{-im\varphi} \int_{-\infty}^{\infty} dz e^{-ik_z z} p(r, \varphi, z). \quad (3)$$

Substituting (2) into (1), we arrive at the Bessel equation for function $P_m(k_z; r)$. Its solutions, corresponding to diverging waves, are expressed by means of the Hankel function: $P_m(k_z; r) = \text{const} H_m^{(1)}(k_r r)$, where $k_r = \sqrt{k^2 - k_z^2}$. As a result, for two arbitrary values of the radial coordinate $r = r_0$ and $r = r_1$, we obtain an expression relating the spatial spectra of acoustic pressure in a diverging wave on different cylindrical surfaces:

$$P_m(k_z; r_1) = \Pi_m(k_z; r_0, r_1) P_m(k_z; r_0), \quad (4)$$

where the factor $\Pi_m(k_z; r_0, r_1)$, often referred to as the “propagator” [10], is expressed by means of the ratio of the corresponding Hankel functions:

$$\Pi_m(k_z; r_0, r_1) = \frac{H_m^{(1)}(\sqrt{k^2 - k_z^2} r_1)}{H_m^{(1)}(\sqrt{k^2 - k_z^2} r_0)}. \quad (5)$$

Thus, if we know the acoustic pressure distribution on any cylindrical surface $r = r_0$, then with the help of expressions (2)–(5), we can calculate what the pressure will be on any cylindrical surface $r = r_1 > r_0$. In contrast, the written expressions make it possible to solve the inverse problem: if we know the pressure distribution at $r = r_1$, then from it we can calculate the initial pressure distribution at the source $r = r_0 < r_1$:

$$P_m(k_z; r_0) = \frac{P_m(k_z; r_1)}{\Pi_m(k_z; r_0, r_1)}. \quad (6)$$

This is the essence of the spectral method of holography of cylindrical sources [8, 11].

In certain cases, what is of interest is not acoustical pressure, but the normal component of vibration speed v_r on the surface of the source. The holographic problem in such a statement is solved in a similar way. From the equation of motion, it follows that the components of the spatial spectrum of acoustic pressure and radial vibration speed are related in the following way: $V_m(k_z; r) = -i(\rho\omega)^{-1} dP_m(k_z; r)/dr$, where ρ is the density of the medium. According to (4) and (5), we have

$$V_m(k_z; r_0) = -i \frac{k_r}{\rho c k} \frac{H_m^{(1)'}(k_r r_0)}{H_m^{(1)}(k_r r_1)} P_m(k_z; r_1), \quad (7)$$

where $H_m^{(1)' }(\xi) = dH_m^{(1)}(\xi)/d\xi$ is an arbitrary Hankel function of the argument. After the spectral amplitude $V_m(k_z; r_0)$ is found, the value of the normal component of vibration speed on the surface of the source is found by inverse Fourier transform:

$$v_r(r_0, \varphi, z) = \frac{1}{2\pi} \sum_{m=-\infty}^{\infty} e^{im\varphi} \int_{-\infty}^{\infty} dk_z V_m(k_z; r_0) e^{ik_z z}. \quad (8)$$

Formulas (3), (7), and (8) allow us to find the velocity distribution on the surface of the source from the results of measuring pressure on the cylindrical surface surrounding it.

The above formulas assign an exact solution to the problem on finding the field at a cylindrical source from the known field at a certain distance from it. However, in implementing the described algorithm in practice, exact calculation proves impossible for several reasons. In addition to the purely technical limit as a result of conducting measurements at a finite number of points, there is a more fundamental problem related to the presence of evanescent (inhomogeneous) waves.

This diffraction feature is well known in the case of plane sources, for which the amplitude of inhomogeneous waves attenuates exponentially with distance.

The presence of noise in the measuring system leads to the fact that the parameters of inhomogeneous waves cannot be measured with sufficient accuracy at large distances from the source. As a result, the above algorithm for solving the inverse problem of finding the field at the source becomes incorrect and its formal application leads to large errors. A practical solution here is to ignore inhomogeneous waves. In such an approach, the problem becomes correct, but inhomogeneities less than the wavelength are not recovered; i.e., the holographic procedure allows us to find only a smoothed variant of the field at the source.

To decrease the effect of smoothing, it is possible to conduct measurements at a relatively small distance from the source, where not all inhomogeneous waves are noticeably attenuated and can therefore be measured and used to find the field at the source (the above-mentioned near-field holography [6]). At present, there are a number of works in which cylindrical sources have been studied by near-field holography. In [8, 11] vibrations of the cylinder in water were studied at frequencies on the order of 2 kHz; as well, special attention was devoted to the presence of inhomogeneous waves with the help of which it was possible to obtain a resolution exceeding the standard diffraction limit. In [12, 13] acoustic sources were studied in air in the presence of noise and inconstancy in the radiation level with the use of near-field holography in cylindrical coordinates in the frequency range of 0.8–1.3 kHz.

In studying piezoelectric sources working at megahertz frequencies, measurements at small distances from the source (on the order of the wavelength) are usually impossible. The reason for this is the inevitable rereflections of an acoustic wave between the receiver and the radiating surface. In addition, electromagnetic interference from the source may be noticeable, masking weak acoustic signals. Therefore, it is necessary to perform measurements at a large distance from the radiator, which makes it impossible to take into account inhomogeneous waves. However, megahertz-range piezoelectric sources used in practice usually have large wave dimensions and the role of inhomogeneous waves in the fields created by them is insignificant. Thus, holography without allowance for inhomogeneous waves is a sufficiently precise tool for studying sources.

For the sources of cylindrically diverging waves considered in this work, inhomogeneous waves have a specific character, allowance for which makes it possible to decrease the effect of diffraction smoothing when performing measurements at large, in comparison to the wavelength, distances. As was already noted, the complex amplitude of the spectral component has the form $P_m(k_z; r) \sim H_m^{(1)}(\sqrt{k^2 - k_z^2} r)$. At $k_z > k = \omega/c$, the argument of the Hankel function becomes imaginary, and it transforms to a Macdonald function of the actual

argument $H_m^{(1)}(i\kappa r) \sim K_m(\kappa r)$, where $\kappa = \sqrt{k_z^2 - k^2}$; i.e., the wave becomes exponentially decreasing: $K_1(\xi)_{\xi \gg 1} \approx \sqrt{\pi/(2\xi)} \exp(-\xi)$. Thus, the spectral components with axial wave number $k_z > k$ describe inhomogeneous waves, which should be discarded in performing measurements at large distances from the source.

However, the condition $k_z \leq k$ is insufficient for the corresponding spectral component to have the form of a diverging wave. Indeed, in the case of plane sources, the angular spectrum component propagates at $\sqrt{k_y^2 + k_z^2} \leq k$, where k_y and k_z are the spatial frequencies in directions y and z on the source plane. By analogy, in the case of cylindrical sources, we can assume the existence of a similar condition in which the role of component k_y should be played by a component corresponding to the polar angle: $k_\varphi = 2\pi/\lambda_\varphi$, where $\lambda_\varphi = 2\pi r/m$ is the spatial period of perturbation at distance r , corresponding to the angular component with index m . In other words, the effective wave number,

$$k_\varphi(r) = m/r, \quad (9)$$

and with it, the condition under which the wave propagates,

$$\sqrt{k_\varphi^2 + k_z^2} \leq k, \quad (10)$$

depend on distance.

This important feature of the behavior of spectral components is not obvious at first glance. Indeed, if the condition $k_z \leq k$ is fulfilled, the argument of the Hankel function as a function of $P_m(k_z; r) \sim H_m^{(1)}(\sqrt{k^2 - k_z^2} r)$ is real; i.e., it is as if the wave is propagating. The seeming paradox is explained by the specific structure of the Hankel function. Note that the Hankel function is expressed by means of the Bessel and Neumann functions: $H_m^{(1)}(\xi) = J_m(\xi) + iN_m(\xi)$. Each of the functions $J_m(\xi)$ and $N_m(\xi)$ entering into this representation is, in contrast to $H_m^{(1)}(\xi)$, a real function and describes a standing cylindrical wave. For Bessel function $J_m(\xi)$, it is known that at $\xi < m$, its value is small; i.e., corresponding field $\sim H_m^{(1)}(\xi) \approx iN_m(\xi)$ turns into a standing wave. In other words, at $\xi = \sqrt{k^2 - k_z^2} r < m$, a wave transfers energy only within the limits of a scale less than the wavelength; i.e., it can be considered non-propagating. Writing this condition in the form $\sqrt{k^2 - k_z^2} < m/r = k_\varphi$, we find that the wave is non-propagating at $\sqrt{k_\varphi^2 + k_z^2} > k$, which coincides with criterion (10) written above for a propagating wave in analogy to the case of plane sources. As was mentioned in [6], attenuation of the mentioned waves occurs approxi-

mately according to a power law: $\Pi_m(k_z; r_0, r) \approx (r_0/r)^m$. Such a dependence means that, although attenuation is rather strong (especially for $m \gg 1$), the drop is not exponentially rapid; i.e., it is possible to record the signal far from the source.

From formulas (9) and (10) it follows that for cylindrical sources it is not always possible to clearly differentiate propagating and nonpropagating waves (in contrast to the case of plane sources). There are three types of waves: (1) permanently propagating components—those for which condition (10) is fulfilled at distance r_0 , i.e., at $k_\varphi = m/r_0$; (2) permanently non-propagating components—those for which $k_z > k$; (3) components that at the source itself and up to a distance of $r = m/\sqrt{k^2 - k_z^2}$ are nonpropagating and then begin to propagate. The existence of the third type of waves results when in a cylindrically diverging wave, the latitudinal scale in the direction in which the polar angle is measured increases linearly with distance; i.e., those inhomogeneities that were initially small in comparison to the wavelength sooner or later begin to exceed the wavelength and therefore cease to rapidly attenuate.

In constructing a far-field holographic algorithm from formula (6), we can use waves of the first type, i.e., permanently propagating spectral components. Such a choice ensures stability but leads to smoothing of pressure propagation at the source both in the z and φ directions. The effect of smoothing of the field at the source in the φ direction can be decreased if we use those waves of the third type that transform to propagating until they have time to noticeably attenuate. However, measurements here can be conducted at distances of many wavelengths from the source, and for accuracy in recovering the field at the source, it is possible to exceed the standard diffraction limit, which is one-half the wavelength (just like in near-field holography).

The criterion for choosing the necessary number of spectral components of the third type depends on the measurement accuracy. As an example, we consider a cylindrical source with a radius $r_0 = 9.25$ mm and a frequency of $f = 1.5$ MHz. Let the holographic information be collected on a cylinder with a radius of $r_1 = 40$ mm; the velocity of sound in the medium is $c = 1.5$ mm/ μ s. Such parameters are used in the numerical experiment described below. In Fig. 2, the dependences of the propagator modulus (5) are constructed for several values of the k_z/k ratio. The values of the critical angular index are

$$m_0(k_z) = \sqrt{k^2 - k_z^2} r_0. \quad (11)$$

When it is exceeded ($m > m_0$), the wave at the source is evanescent, it corresponds to the vertical dashed line. As is seen, with increasing angular index, the propagator hardly subsides at all up to m_0 , but the incipient

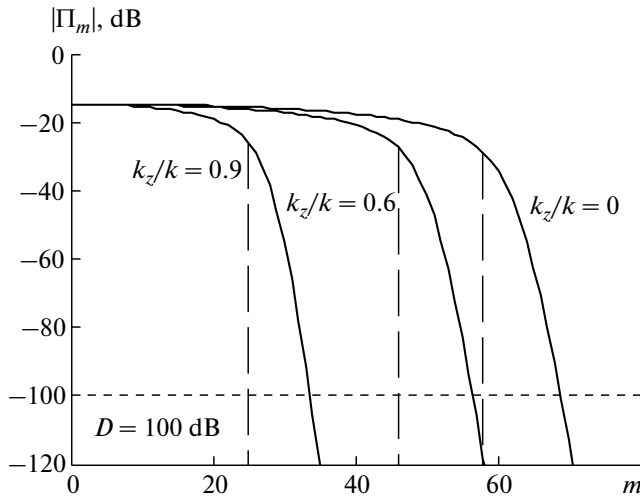


Fig. 2. Dependence of quantity $20 \log |\Pi_m|$ on m , where $\Pi_m(k_z; r_0, r_1)$ is propagator (5), for values of $r_0 = 9.25$ mm, $r_1 = 40$ mm, $f = 1.5$ MHz, and for $k_z/k = 0, 0.6$, and 0.9 . Vertical dashed lines correspond to values of the critical angle index $m_0(k_z) = \sqrt{k^2 - k_z^2} r_0$, which when exceeded ($m > m_0$), the wave at the source is nonpropagating.

(upon further growth m) drop is not steep, owing to which on the surface $r = r_1$, part of the spectral components with numbers $m > m_0$ can be recorded. For instance, at $k_z/k = 0$, 100 dB attenuation occurs at $m \approx 1.17m_0$. Thus, in finding the field at the source, we can use a larger number of angular components and in the same way increase the spatial resolution.

We consider a numerical example illustrating the features of the examined holographic algorithm. Let at the initial cylinder with radius $r_0 = 9.25$ mm the pressure differ from zero on one-half of the cylinder ($\pi/2 \leq \varphi \leq 3\pi/2$) within the limits of a region with a height of $l_0 = 6$ mm ($7 \text{ mm} \leq z \leq 13 \text{ mm}$); see Fig. 3a. The radiation frequency $f = 1.5$ MHz. Let the amplitude and wave phase be measured on a cylinder with a radius of $r_1 = 40$ mm and a height of $l = 20$ mm ($0 \leq z \leq 20$ mm). Measurements are conducted in mesh nodes with a step (0.25 mm) less than a half-wavelength (0.5 mm).

The calculation algorithm is explained in Fig. 3. As a first step, from formula (3) using a step much less than the wavelength with the help of fast Fourier transform (FFT), we calculated the spatial spectrum of the

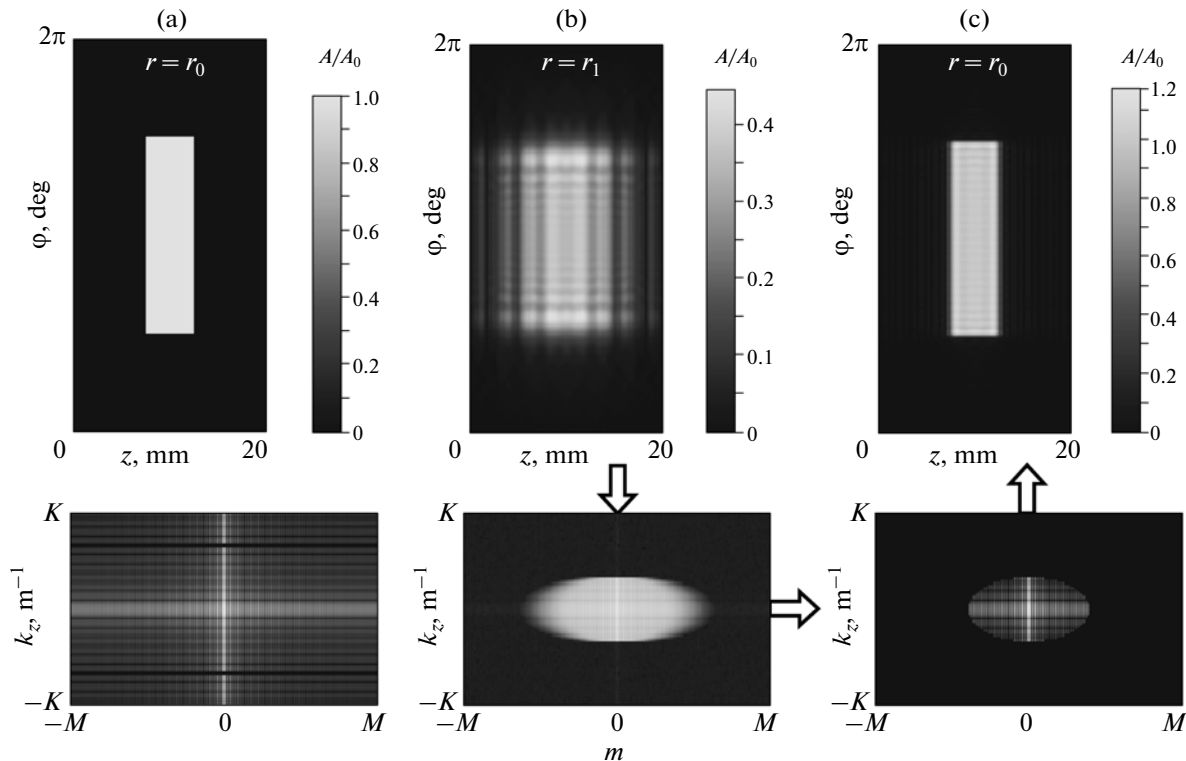


Fig. 3. Amplitude distribution of acoustic pressure (top) and corresponding spatial spectrum in a logarithmic scale (bottom). Boundaries of the spectral region: $K = 12.6 \times 10^3 \text{ m}^{-1}$, $M = 120$. (a) Initial distributions on the surface of the model cylindrical radiator with a radius of $r_0 = 9.25$ mm and a height of $l = 20$ mm at a frequency of $f = 1.5$ MHz. (b) Pressure distribution and spectrum on the measurement surface $r_1 = 40$ mm. (c) Recovered pressure distribution and spectrum on the radiator surface.

pressure field at the source $P_m(k_z; r_0)$; see Fig. 3a, lower panel. Then, from formulas (4), (5), we found the spatial spectrum $P_m(k_z; r_1)$ on the measurement surface $r = r_1$. At the next step, from formula (2) we calculated the values of pressure $p(r, \varphi, z)$ at the nodes of the measurement mesh. This distribution simulated data of a hypothetical experiment (Fig. 3b, top). Further, we use these data to calculate the spatial spectrum $r = r_1$ on the basis of formula (3), in which the intervals were approximately replaced by sums from the method of rectangles. We calculated only those spectral components for which attenuation in the region from $r = r_0$ to $r = r_1$ is not too large (i.e., either only propagating waves or, in addition to it, the discussed waves of mixed type). The amplitude of the remaining components were taken to be equal to zero. The obtained distribution is shown in Fig. 3b, bottom. After this, from formula (6), we solved the inverse problem: we found the spatial spectrum of the wave at the source, i.e., at $r = r_0$ (Fig. 3c, bottom). Further, from formula (2), in which integration was approximately replaced by summation, we calculated the pressure distribution at the source (Fig. 3c, top), which we compared to the initial value $p(r_0, \varphi, z)$ (Fig. 3a, top). With deviation of the calculated distribution from the initial one, we could estimate the accuracy of holographic recovery and find the appropriate parameters of the measurement mesh.

BACK PROPAGATION METHOD BASED ON THE RAYLEIGH INTEGRAL

The indicated method was described by us earlier for studying plane and spherically focused radiators [2, 3] possessing a clearly expressed direction characteristic. We briefly state the essence of the method. At a certain distance from the studied acoustic source, we consider the surface enveloping it Σ_H , the acoustic pressure at which is considered known from experiment. The fields of quasi-plane sources of large wave dimensions have the form of beams limited in the latitudinal direction, and therefore in practice it is sufficient to perform measurements in the region of the surface opposite the source. The problem lies in finding the acoustic characteristics on the surface of a harmonic source using a hologram—the distribution, measured in region Σ_H , of the complex amplitude of acoustic pressure $p_H(\mathbf{r}')$, where \mathbf{r}' are the coordinates of points of the surface Σ_H . The fundamental possibility of this follows from the reversibility of the wave equation in time. If surface Σ_H can be ideally replaced by a mirror reversing time (in the case of harmonic waves, reversing phase), then the wave reflected from it will propagate backwards and, reaching the source, in a certain sense will recover its initial characteristics. The amplitude of the normal component of the vibra-

tion speed at point \mathbf{r} on the surface of the source $v(\mathbf{r})$ can be calculated from the pressure amplitude $p_H(\mathbf{r}')$ using a Rayleigh-type integral [3]:

$$v(\mathbf{r}) = \int_{\Sigma_H} p_H(\mathbf{r}') K(\mathbf{r}, \mathbf{r}') dS' \quad (12)$$

with the kernel

$$K(\mathbf{r}, \mathbf{r}') = \frac{1}{2i\pi\omega\rho} \frac{\partial^2}{\partial \mathbf{n} \partial \mathbf{n}'} \left(\frac{\exp\left[-i\frac{\omega}{c}|\mathbf{r} - \mathbf{r}'|\right]}{|\mathbf{r} - \mathbf{r}'|} \right). \quad (13)$$

Here, $\mathbf{n} = \mathbf{n}(\mathbf{r})$ is the unit external normal to the surface of the source at recovery point \mathbf{r} , and $\mathbf{n}' = \mathbf{n}'(\mathbf{r}')$ is a unique normal to surface element $dS' \in \Sigma_H$ oriented in the direction of the source. If we designate $R = |\mathbf{r} - \mathbf{r}'|$ and $\mathbf{e}_R = (\mathbf{r} - \mathbf{r}')/R$, then after differentiation, the expression for kernel (13) takes the form

$$K(\mathbf{r}, \mathbf{r}') = \frac{\exp\left[-i\frac{\omega}{c}R\right]}{i2\pi\omega\rho} \left[(\mathbf{n} \cdot \mathbf{n}') \left(\frac{1}{R^3} + \frac{i\omega}{cR^2} \right) - (\mathbf{n} \cdot \mathbf{e}_R) \cdot (\mathbf{n}' \cdot \mathbf{e}_R) \left(\frac{3}{R^3} + \frac{3i\omega}{cR^2} - \frac{\omega^2}{c^2 R} \right) \right]. \quad (14)$$

Note that the above-described holographic method is approximate. The reason for this is the fundamental circumstance that the invariance of the wave equation relative to the change in sign of time is insufficient for full reversal of the wave process in time [14, 15]. In a strict calculation of the back propagation, it is also necessary to do it such that the boundary conditions are reversed in time; i.e., all sources become sinks equal in magnitude. In calculating waves by formula (12) on the surface of a radiator, no sinks arise. Instead of this, a back-propagating (hypothetical) wave is rendered the ability to freely pass through the surface of the radiator, which only approximately replaces the sinks located there, especially if holographic recovery of small (in comparison to the wavelength) field inhomogeneities on the radiator take place. As a consequence, in calculating the field distribution at the radiator by formula (12), diffraction smoothing of inhomogeneities less than the wavelength occurs. At the same time, for large field inhomogeneities at the radiator, replacement of sinks by “transparency” of the surface is quite justified, which explains the high accuracy of the method for quasi-plane sources of large wave dimensions.

In this paper, we consider cylindrical sources of large wave dimensions, for which there is spatial localization of the field only in the direction along the cylinder axis, and in the plane, along the perpendicular axis, radiation diverges in all directions. Due to the indicated features, as a measurement surface Σ_H for recording the entire radiated field, it is necessary to

take a surface that encloses the studied source from all sides at the polar angle. In calculating back propagation according to formula (12), from such a surface closed by the polar angle, a wave intersects each element of the surface of a cylindrical radiator twice—not only externally, but also internally; i.e., not only the necessary sinks effectively arise, but parasitic sources. Therefore, Rayleigh integral (12) does not permit a correct recovery of the field on the radiator surface.

We can make a necessary modification to the method based on allowance for the limiting case of very high frequencies, when wave propagation occurs in accordance with the geometric acoustics approximation. In this approximation, during back propagation, waves not from all surface Σ_H elements arrive at a given point, but only from those not shielded by the cylindrical radiator itself. The remaining surface Σ_H elements are in the acoustic shadow zone. Therefore, if we exclude them in calculation by formula (12), then the above-mentioned parasitic sources will also be excluded. In such an approach, we should take Rayleigh integral (12) as the basis for holography; in this integral, integration is done not over entire measurement surface Σ_H , but only over that part of it $\sigma_H(\mathbf{r}) \in \Sigma_H$ that is visible from point \mathbf{r} of the radiator surface. If the radiator surface is a cylinder of radius r_0 , the field is recovered at a point with angular coordinate φ , and holographic information is collected on the cylindrical surface of radius r_1 , then the indicated surface σ_H corresponds to the range of changes in polar angle $\varphi \pm \arccos(r_0/r_1)$. Formula (12) in this approximation takes the form

$$\begin{aligned} v(r_0, z, \varphi) = & \int_{\varphi - \arccos(r_0/r_1)}^{\varphi + \arccos(r_0/r_1)} r_1 d\varphi' \\ & \times \int_{z_{\min}}^{z_{\max}} dz' p_H(r_1, z', \varphi') K(z - z', \varphi - \varphi'). \end{aligned} \quad (15)$$

Here, z_{\min} and z_{\max} give the borders of the interval of changes in the axial coordinate in the scanning region and kernel (14) is described by the following expression:

$$\begin{aligned} K(\zeta, \psi) = & \frac{i}{2\pi\rho c} \frac{e^{-ikR}}{kR^2} \left[\cos\psi \left(\frac{1}{R} + ik \right) \right. \\ & \left. + (r_0 - r_1 \cos\psi)(r_1 - r_0 \cos\psi) \left(\frac{3}{R^3} + \frac{3ik}{R^2} - \frac{k^2}{R} \right) \right], \end{aligned} \quad (16)$$

where $k = \omega/c$ is the wave number and $R = \sqrt{r_0^2 + r_1^2 - 2r_0r_1 \cos\psi + \zeta^2}$.

In the experiment, the parameters of acoustic waves are measured in a finite set of points of surface Σ_H ; therefore, when expression (15) is used, the inte-

gral should be approximated by a sum. When the method is used in practice, in collecting holographic information (i.e., in measuring the amplitude and phase of the wave), the choice of the scanning step is extremely important. At too high a step, the parameters of the field at the radiator are recovered with a significant error. If the step is chosen too small, in order to guarantee extra recovery accuracy, then the scanning time can prove inadmissibly large (more than several hours). It is natural to choose a scanning step based on the requirement that at the magnitude of the step the measured field changes little. This requirement is deliberately fulfilled at a half-wavelength step (the corresponding criterion is none other than the Nyquist criterion arising in the analysis of the spatial spectrum). In the case of cylindrical sources at a distance of many wavelengths, the diagram of the directional characteristic is established and the angular measurement scale of the field therefore does not change; i.e., the spatial scale increases in proportion to distance from the source. Therefore, a linear step in the direction of change in angle can be increased in accordance with the required angular step $\Delta\varphi = \lambda/(2r_0)$. The scanning step along the source taxes should be taken close to the half-wavelength. Larger steps can also prove insufficient, especially if the scanning surface is close to the phase front of the wave. To find the most admissible step, it is convenient to perform numerical simulation of direct and back propagation problems as applied to a specific radiator.

The results of calculations and comparison of the suggested holographic method with the spectral method are described below.

EXPERIMENT

To check the described holographic methods, we conducted a number of experiments with cylindrical sources in water. Below we give the results for two sources, the first of which was analyzed by the spectral holographic method, and the second, by the Rayleigh integral method. Both sources were cylindrically shaped and were prepared from a radially polarized PZT piezoceramic.

The first radiator was a cylinder with an external diameter of 18.5 mm, a width of 1 mm, and a height of 20 mm. The internal part of this ceramic cylinder was filled with air. The radiator was attached to the end face of a vertically situated metal rod coaxial with it, which was able to turn in a controlled manner around the axis and shift along the axis via a micropositioning system (Velmex UniSlide VP9000, United States). Before conducting the experiment, coincidence of the axis of rotation and the radiator axis was ensured with an accuracy of up to 0.05 mm by means of a preliminary setup and control of the gap between the surface of the rotating cylinder and an immobile screen with the aid of a set of calibration probes. To measure pres-

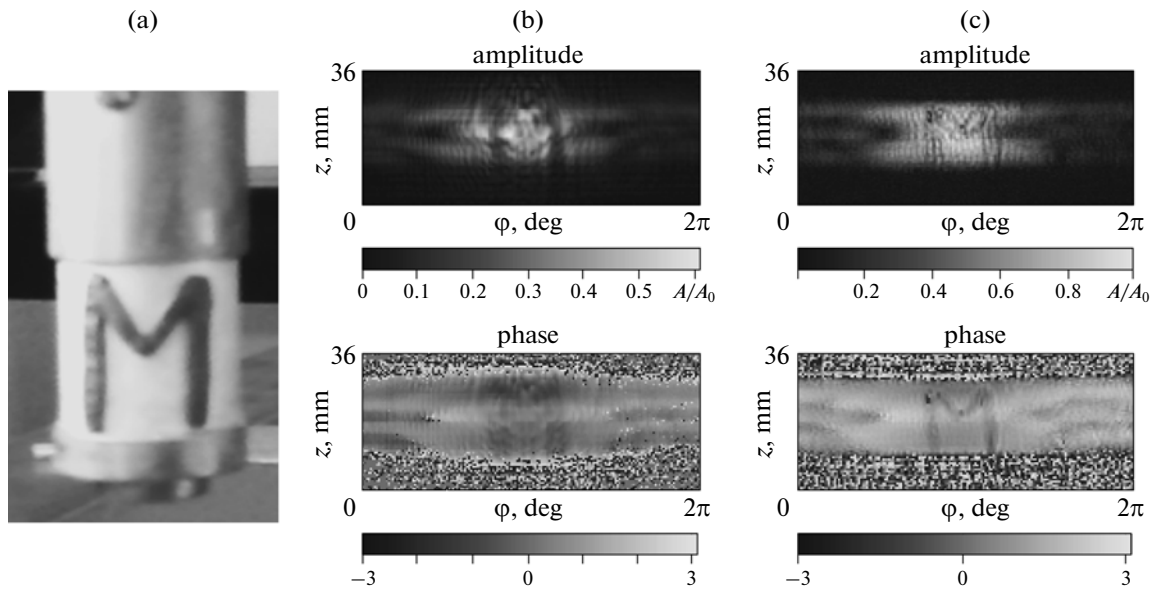


Fig. 4. (a) Photograph of the radiator, $r_1 = 9.25$ mm, $l = 20$ mm, $f = 1.528$ MHz; (b) amplitude and phase distribution of pressure on the measurement surface, $r_1 = 40$ mm; (c) recovered amplitude and phase distribution of pressure on the radiator surface.

sure, a needle-shaped hydrophone (SEA, PVDFZ44-0400) with a preamplifier was used, with the diameter of the sensitive region of 0.4 mm, which was also submerged in water and fixed at a given distance from the source. During scanning, the hydrophone was immobile and the cylindrical source was turned over or shifted in the vertical direction. Such scanning in the coordinate system of the source was equivalent to displacement of the sensor along the cylindrical surface surrounding the studied source. Voltage to the radiator was fed from a generator (Hewlett Packard 33120A) in the form of radio pulses with a duration of 50 μ s and a modulation frequency of 0.7–1.5 MHz (for different radiators). The pulse repetition rate was about 300 Hz. The signal from the hydrophone passed through the amplifier to the oscilloscope (Tektronix TDS520A), after which it was processed by a computer. To increase the signal-to-noise ratio, which determines the quantity D , in addition to amplification of the signal fed to the radiator, averaging of the received signal was performed over several periods (10–20) within the limits of the observed time window and over time (0.5–5 s) at a fixed sweep frequency of 300 Hz at every point in space. By increasing the time of averaging, it is possible to achieve values of $D = 150$ dB or higher; however, the total measurement time in this case for a scanning array of 360×100 points should be several days. In the operating mode with parameters of averaging at which full scanning was conducted over a time of 6–8 h, quantity D is equal to values from 60 to 80 dB. The radiator was displaced stepwise by a computer-controlled positioning system.

Figure 4a shows the external view of the radiator with parameters $r_0 = 9.25$ mm, $l = 20$ mm, $f =$

1.528 MHz with a plasticine “M” affixed to the radiating surface. Figure 4b shows the distribution of amplitude (top) and phase (bottom) of acoustic pressure on the cylindrical surface with radius $r_1 = 40$ mm. Measurements were performed on a mesh of 360×80 points with an angular step of 1 deg in the direction of the radiator axis with a step of 0.5 mm. The measured field contains information on the acoustic pressure distribution on the radiator surface, including the strongly blurred contour of the “M.” Figure 4c shows the distributions of amplitude and phase of acoustic pressure on the surface of a cylindrical source obtained by the described spectral method of acoustic holography. In calculations, we used the restriction on the spatial spectrum of the signal using the value $D = 80$ dB. It is distinctly seen that the characteristic features of the amplitude and phase distribution of pressure well replicates shape of the affixed letter “M.”

Data for this radiator were processed by the Rayleigh integral. Pictures of the amplitude and phase distribution of pressure on the surface of the source obtained by the two methods proved practically indistinguishable. Therefore, here we only give results obtained by the angular spectrum method. A more detailed comparison of the two methods is given in the concluding section of the paper.

The second cylindrical source had a height of 6 mm and a diameter of 2.7 mm. The wall thickness of the cylinder was 270 ± 25 μ m. In the inner cavity of the cylinder, there was an acoustic reflector—a brass rod separated from the inner wall of the cylinder by a water space slightly less than a half-wavelength. The source achieved maximum acoustic power in the frequency

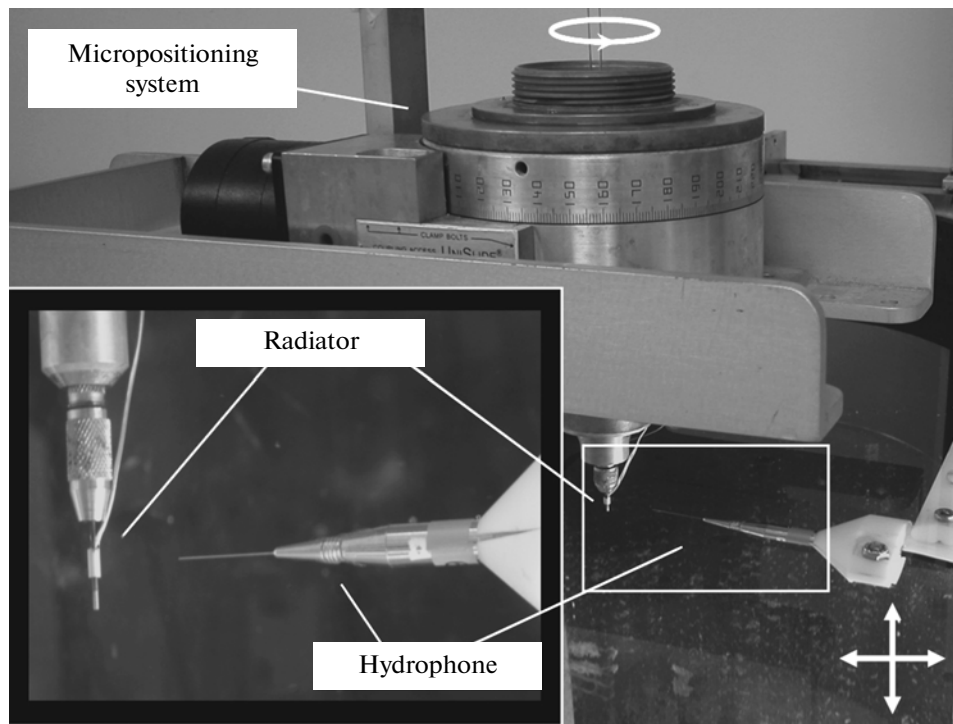


Fig. 5. Photograph of the setup for scanning cylindrical radiators. The needle-shaped hydrophone can be shifted by a micropositioning system, and the radiator can be turned around its own axis. The source and receiver are located in a water tank.

band near 9.0 ± 0.25 MHz. It was placed on the end of an intravascular catheter designated for minimum invasive action on heart tissues in treating symptoms of auricle arrhythmia [16].

Just like in the case of the first radiator, the ultrasound field was measured in the pulse-periodic mode. We used a ProRhythm Inc (United States) micropositioning setup for quality control of the radiators (depicted in Fig. 5). The tip of the catheter with the cylindrical radiator positioned on it was turned about its own axis, and the hydrophone moved independently in the axial (vertical) direction. This enables the measurement of acoustic pressure at random points coaxial with the radiator over the cylindrical surface. Rotation of the radiator and shifting of the hydrophone was carried out automatically by the computer-controlled step motors of the micropositioning system. Electric pulses 5–10 μ s in duration were generated by an HP 33120A generator (Agilent Technologies Inc, United States), amplified by a Communication Power Corporation amplifier (Hauppauge, NY, United States) and fed to the radiator. The mean electrical power did not exceed 30 W at a pulse repetition rate of 1 kHz. Each radiating acoustic signal was received by a miniature needle-shaped hydrophone with a diameter of the sensitive region of 40 μ m (Precision Acoustics Ltd, Dorchester, United Kingdom). The electrical signal of the hydrophone was fed to the input of the oscilloscope (HP 54615B, Agilent Technologies Inc, United

States), where in the given time window, a constant-in-amplitude part of the signal was averaged. The corresponding time region was transferred into a computer, and, with the help of the Hilbert transform, the amplitude and phase shift of acoustic pressure was calculated relative to a reference signal with the same carrier frequency.

The distribution of the normal velocity component on the radiator surface was calculated by the holographic method using the Rayleigh integral from formulas (15), (16). Note that, since the frequency of the source was comparatively high, the size of analyzed inhomogeneities was much larger than the wavelength; i.e., there was no need to increase the resolution using inhomogeneous waves. Therefore, in analyzing the data, the angular spectrum method was not used (in contrast to the previous experiment). The results of conducting measurements at distances from 10 to 60 mm coincided and depended little on the system alignment. Below, we give results for scanning at a frequency of 9 MHz at a distance of $r_1 = 20$ mm. Vertical scanning was performed within the limits of 12 mm (i.e., at an interval higher than the height of the source by a factor of 2) with the step of 0.1 mm, which is several times smaller than the wavelength in water, $\lambda = 0.167$ mm. Scanning along one vertical line took almost a minute, and the overall scanning time, proportional to the number of angular steps, was from 1 h (60 steps at 6 deg) to several hours. Note that the scale for one wavelength

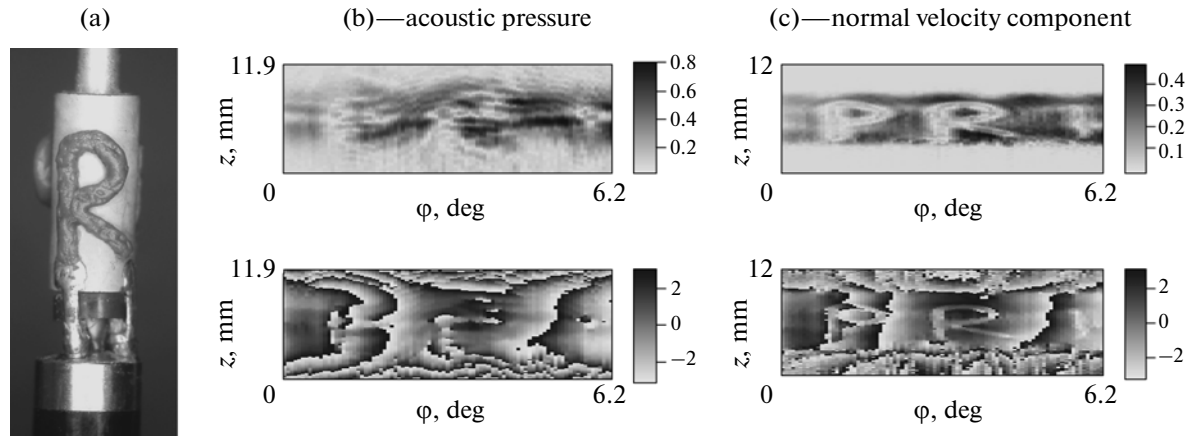


Fig. 6. (a) Photograph of the radiator. (b) Amplitude (top) and phase (bottom) distribution of acoustic pressure on the measurement surface, $r_1 = 20$ mm. (c) Recovered amplitude and phase distribution of pressure on the radiator surface, $r_0 = 1.35$ mm. Scales for the amplitude of acoustic pressure and velocity are given, respectively, in MPa and m/s.

normalized to the surface of the source corresponds to approximately 7 deg.

Figure 6a shows the external view of the radiator. On the surface of the radiator, an absorption band of wax in the shape of the Latin letters “PRI” has been applied. Similarly to Figs. 4b and 4c, Fig. 6b shows the amplitude (top) and relative phase (bottom) distributions, and Fig. 6c shows the distribution of the normal component of the vibration speed on the surface of the radiator. In contrast to the previous experiment, the velocity distributions in the given case were obtained by the back propagation method based on Rayleigh integral (15). The contours of the letters “PRI” are distinctly recognized in the recovered velocity distribution in Fig. 6c, but differ little in the amplitude and phase distribution on the measurement surface (Fig. 6b). The simplicity and stability of the method made it possible to accumulate significant experience of a holographic visualization of various surface, solder, and crack defects, as well as other inhomogeneities, and over time to develop a reliable quality control system of manufactured radiators at their final stage.

DISCUSSION AND CONCLUSIONS

Radiation of cylindrical sources diverge in all directions from the source axis. This feature should be taken into account in formulating various methods of acoustic holography.

In particular, if, in using the spatial spectrum method, we act in analogy to the case of plane sources, then holography can prove either impossible or insufficiently exact. This primarily concerns the choice of maximum angular index m , retained in the expansion over spatial harmonics (2). If we use all possible spectral components, which are propagating waves on the scanning surface, then in calculating back propagation, instability arises. This is related to the fact that

when the source is approached, certain retained components of the spatial spectrum transform into rapidly attenuating (inhomogeneous) waves, and the problem of back propagation of such waves becomes incorrect. The back propagation algorithm will be deliberately stable if we choose the maximum angular index such that all retained spectral components will be propagating at the same source. However, in this case, the highest accuracy will not be achieved, because at the given cutoff, the informative high-quality part of the spatial spectrum is not used, which corresponds to transition-type waves, those which are initially inhomogeneous but at a certain distance from the source change their type and begin to propagate without strong attenuation. The optimal cutoff frequency in the same way lies between the two indicated characteristic frequencies.

In the acoustic holography of cylindrical sources based on use of the Rayleigh integral, there is also a certain specific character in comparison to the case of plane sources. This is the fact that in calculating back propagation, integration is performed not over the entire measurement surface enclosing the source, but only over the part of it that is visible from the studied point of the source.

The spatial resolution of all of the above-described holographic methods are limited by diffraction. In practice, this means that in holographic recovery, small-scale field inhomogeneities are lost; i.e., smoothing occurs. The question is quite logical to what extent effective diffraction smoothing distorts the true field at the source when various holographic methods are used. Qualitatively, the answer to this question is obvious: smoothing should manifest itself for inhomogeneities on the order of the wavelength or smaller. For a quantitative description, it is necessary to simulate back propagation.

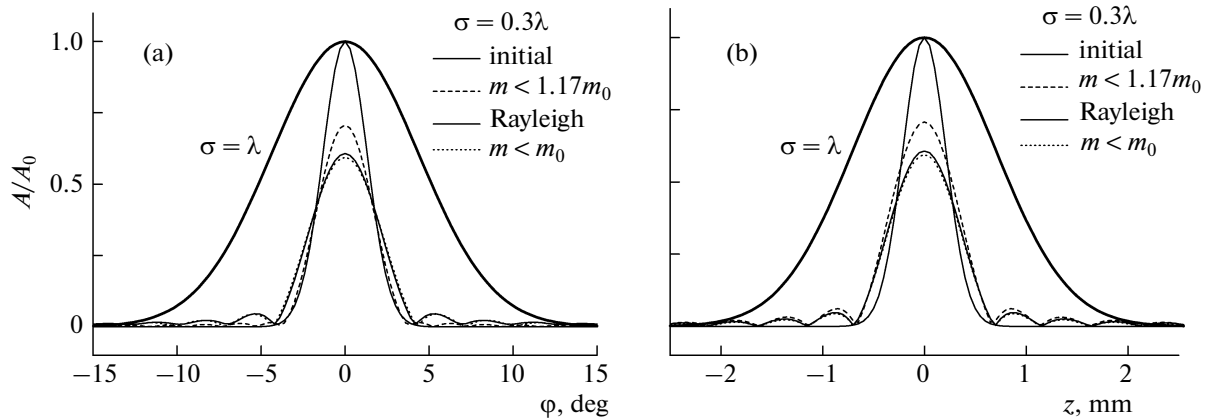


Fig. 7. Pressure distribution on the surface of a cylindrical radiator with a radius of $r_1 = 9.25$ mm and the angular (a) and axial (b) directions. The initial distribution is given by the Gauss distribution $\exp[-(z^2 + r^2\varphi^2)/\sigma^2]$ for $\sigma = 0.3\lambda$ and $\sigma = \lambda$ at $\lambda = 1$ mm. Given are the initial distribution and result of recovery from the measurement surface $r_1 = 40$ mm by the Rayleigh integral method and the spectral method at $m < m_0$ and $m < 1.17m_0$. For $\sigma = 0.3\lambda$, the recovery curves differ noticeably, and for $\sigma = \lambda$, all curves merge and coincide with the initial distribution.

It is convenient to examine inhomogeneity in the form of a small active region on the surface of the cylindrical source. We consider the case of the Gaussian profile of acoustic pressure $\sim \exp[-(z^2 + r^2\varphi^2)/\sigma^2]$ in axial and angular coordinates. Here, σ is the characteristic diameter of the active region.

Figure 7 shows the initial Gaussian distributions as a result of their recovery when different holographic approaches are used for the cases $\sigma = \lambda$ and $\sigma = 0.3\lambda$; the parameters of the cylindrical radiator are indicated in the caption. On the left are the angle distributions; on the right, axial coordinate distributions. Calculation was performed by the Rayleigh integral method, as well as the spatial spectrum method using permanently propagating components ($m \leq m_0$) and with additional allowance for transition-type waves ($m \leq 1.17m_0$). It is noteworthy that with a size of an inhomogeneity equal to the wavelength ($\sigma = \lambda$), all holographic methods give virtually ideal recovery. As is seen in Fig. 7, all corresponding curves merge with the initial distribution. Thus, already beginning with inhomogeneities of the size of the wavelength, any of the considered methods can be considered exact. Diffraction features manifest themselves only for smaller inhomogeneities. This is seen from comparison of curves at $\sigma = 0.3\lambda$. All methods give a certain surface vibration pattern reconstruction error. The most accurate reconstruction occurs when the spatial spectrum is used with retention of transition-type components ($m \leq 1.17m_0$). The spatial spectrum method using permanently propagating components and the Rayleigh integral method give virtually identical distributions. In other words, in practice, with equal justification it is possible to use both variants of acoustic holography. It is important that all of them enable to find the surface vibration distribution

at the source with high accuracy, which is limited only by the effect of smoothing of inhomogeneities smaller than the wavelength.

ACKNOWLEDGMENTS

The work was partially supported by grants from the Russian Foundation for Basic Research (project no. 08-02-00368-a), ISTC 3691, NIH R01EB007643, and NSh- 4590.2010.2.

REFERENCES

1. D. Cathignol, O. A. Sapozhnikov, and J. Zhang, *J. Acoust. Soc. Am.* **101**, 1286 (1997).
2. O. A. Sapozhnikov, A. V. Morozov, and D. Cathignol, in *Proc. of the IEEE Int. Ultrason. and UFFC 50th Anniv. Joint Conf.* (2004), pp. 161–164.
3. O. A. Sapozhnikov, Yu. A. Pishchal'nikov, and A. V. Morozov, *Akust. Zh.* **49**, 416 (2003) [*Acoust. Phys.* **49**, 354 (2003)].
4. O. A. Sapozhnikov, A. E. Ponomarev, and M. A. Smailin, *Akust. Zh.* **52**, 385 (2006) [*Acoust. Phys.* **52**, 324 (2006)].
5. Y. D. Sinel'nikov, T. Fjield, and O. A. Sapozhnikov, *Akust. Zh.* **55**, 641 (2009) [*Acoust. Phys.* **55**, 647 (2009)].
6. E. G. Williams, *Fourier Acoustics: Sound Radiation and Nearfield Acoustical Holography* (Academic, London, 1999).
7. E. G. Williams and J. D. Maynard, *Phys. Rev. Lett.* **45**, 554 (1980).
8. E. G. Williams, H. D. Dardy, and K. B. Washburn, *J. Acoust. Soc. Am.* **81**, 389 (1987).
9. V. K. Alekseev and L. F. Lependin, *Akust. Zh.* **14**, 126 (1967) [*Sov. Phys. Acoust.* **14**, 97 (1967)].

10. X. Zeng and R. J. McGough, *J. Acoust. Soc. Am.* **123**, 68 (2008).
11. E. G. Williams, B. H. Houston, and J. A. Bucaro, *J. Acoust. Soc. Am.* **86**, 674 (1989).
12. M. Lee and J. S. Bolton, *J. Acoust. Soc. Am.* **118**, 3721 (2005).
13. M. Lee and J. S. Bolton, *J. Acoust. Soc. Am.* **119**, 382 (2006).
14. M. Fink, in *Nonlinear Acoustics at the Turn of the Millennium: ISNA15*, Ed. by W. Lauterborn and T. Kurz (Amer Inst. Phys., New York, 2000), pp. 33–34.
15. V. A. Zverev, *Akust. Zh.* **50**, 685 (2004) [*Acoust. Phys.* **50**, 523 (2004)].
16. Y. Sinelnikov, A. Vedernikov, and O. Sapozhnikov, in *Proc. of the UIA 2007 Symp.* (2007), p. 11.

Translated by A. Carpenter